

Equivalent Circuit for the Leakage Inductance of Multiwinding Transformers: Unification of Terminal and Duality Models

Casimiro Álvarez-Mariño, Francisco de León, *Senior Member, IEEE*, and Xosé M. López-Fernández, *Member, IEEE*

Abstract—In this paper, a new equivalent circuit for the leakage inductance of multiwinding (or multisection) transformers is presented. The methods proposed in this paper unify terminal models with models derived from the principle of duality between electric and magnetic equivalent circuits. The new model is identified as the terminal-duality model (TDM). The elements of the circuit in addition to properly representing the transformer behavior at the terminals are physically related to flux paths in the transformer window. The circuit of the TDM consists of a set of mutually coupled inductors available in any circuit simulation program and, in particular, available in all Electromagnetic Transients Program-type programs. The circuit elements of the TDM can be computed in two ways: 1) from the observation of the behavior of the magnetic field in the transformer window (applying the principle of duality) and 2) from measurements on short-circuit tests performed at the transformer terminals. Both methods yield identical results. The 2-D finite-element simulations are used to compute the terminal behavior of a wide variety of winding configurations. Several examples are presented for the illustration of the model capabilities and validation.

Index Terms—Duality model, leakage impedance, leakage inductance, terminal model, transformer equivalent circuit.

I. INTRODUCTION

TRANSFORMER models used for steady-state studies do not have enough accuracy for the computation of electromagnetic transients [1]. Models exist that are sufficiently accurate for the calculation of low-frequency transients (less than 1 kHz) using time-domain simulations [1]–[3]. At a low-frequency range, not only does the electromagnetic field fully penetrate the windings, but also there is no need to subdivide a winding into sections since the wavelength is very large. Similarly, relatively good models for the simulation of very-high frequency transients (>1 MHz) are also available [1], [4]–[18]. At very-high frequency, the magnetic flux does not penetrate the windings and, consequently, there is no need to represent the eddy currents dynamically. The challenge that

all transformer modelers face is the accurate estimation of the model parameters.

Only a few models exist for the mid- to high-frequency range, where the dynamics of eddy currents need to be represented in detail. The most advanced time-domain model for studies in this frequency range was presented in [19] (derived from [20]). It is capable of correctly representing the dynamic behavior of the eddy currents in the winding over a wide frequency range [21]. However, it is not widely used, perhaps because it does not have a standard equivalent circuit representation with components available in Electromagnetic Transients Program (EMTP)-type programs. Recently, Del Vecchio [22], [23] has extended the model of [20] to multiterminals by using two winding leakage inductances. This was further developed to three-winding transformers in [24], relying on coupled equivalent circuits.

The contribution of this paper is the generalization of the model of [24] applied to multisection windings effectively unifying terminal models with duality derived models. The new model is labeled as the terminal-duality model (TDM). The TDM consists of a set of mutually coupled inductors that are readily available in all EMTP-type programs. Each self-inductor in the model physically represents a path of leakage flux in the transformer window.

A series of examples is presented to illustrate the derivation, use, and capabilities of the TDM. Validation is carried out with finite-element simulations in 2-D and, when possible, with existing analytical formulas for simplified geometries.

II. LEAKAGE INDUCTANCE AND TESTS

The parameters of the proposed TDM can be calculated from the standard impedance voltage tests [25] and nonstandard short-circuit admittance tests. The former, the standard impedance voltage tests, is carried out between a pair of windings (for example, winding i and winding j). While winding i is energized, winding j is short-circuited, keeping the remaining windings in open circuit (Test $_{i,j}$) as shown in Fig. 1(a). From this test, the leakage impedance between two windings $Z_{s_{i,j}}$ is calculated as (By neglecting the resistance, one can obtain the leakage inductance $L_{s_{i,j}}$)

$$Z_{s_{i,j}} = \left. \frac{U_i}{I_i} \right|_{U_j=0, I_q=0} = j\omega L_{s_{i,j}}; i \neq j; q \neq i, j; i, j, q = 1, \dots, n. \quad (1)$$

U_i is the voltage source connected to the winding i , I_i is the current flowing through the winding i , I_q is the current flowing through the other windings, n is the number of coils per phase,

Manuscript received June 06, 2011; revised October 04, 2011; accepted October 11, 2011. Date of publication December 05, 2011; date of current version December 23, 2011. Paper no. TPWRD-00489-2011.

C. Álvarez-Mariño and X. M. López-Fernández are with the Department of Electrical Engineering, Universidade de Vigo, Vigo 36310, Spain (e-mail: csmalvarez@uvigo.es; xmlopez@uvigo.es).

F. de León is with the Department of Electrical and Computer Engineering, Polytechnic Institute of New York University, Brooklyn, NY 11201 USA (e-mail: fdeleon@poly.edu).

Color versions of one or more of the figures in this paper are available online at <http://ieeexplore.ieee.org>.

Digital Object Identifier 10.1109/TPWRD.2011.2173216

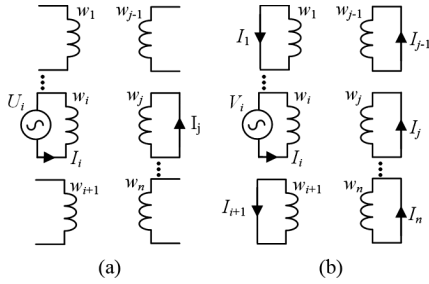


Fig. 1. (a) Standard leakage impedance tests on a multiwinding transformer. (b) Short-circuit admittance tests on a multiwinding transformer.

and $j\omega$ is the operator complex affected by the angular frequency. This test is made for all of the $n \cdot (n - 1)/2$ possible combinations of pairs of windings.

In the nonstandard short-circuit admittance tests, winding i is energized while the other windings are short-circuited as shown in Fig. 1(b). From this test, the short-circuit admittance Y_{ij} is calculated as follows:

$$Y_{ij} = \frac{I_j}{V_i} \Big|_{V_k=0} \quad k \neq i; \quad i, j, k = 1, 2, \dots, n. \quad (2)$$

V_i is the voltage source connected to winding i , I_j is the current flowing through winding j , and n is the number of coils per phase.

The previously described tests can be performed on a real transformer in two ways: (1) by simulation, for example, by using a finite-element model (FEM) or, (2) by means of laboratory measurements. Thus, a 2-D-FEM simulation for computing leakage impedances and short-circuit admittances tests is developed. The commercial software package Flux 2D is used [26] in all examples in this paper.

A 2-D model of a five concentric layer transformer (see Fig. 2) is implemented in order to check the validity of the FEM simulations. The leakage inductances obtained by the 2-D-FEM simulations are collected in Table I and the resulting currents, when a voltage source of 1 V is applied, are shown in the second column of Table II. The numerical values are validated with analytical results obtained by applying the well-known design formula [27]:

$$L_{s_{i,j}} = \frac{\mu_0 N_i^2}{ls} \left(2\pi r_\delta \delta + \frac{2\pi r_i a_i + 2\pi r_j a_j}{3} \right) \quad (3)$$

where μ_0 is the permeability of vacuum, N_i is the number of turns of winding i , ls is the height of the windings, a_i and r_i are the width and radius of winding i ; and δ and r_δ are the width and radius of the dielectric space between windings j and i .

From Table I, one can confirm that the differences between the numerical and analytical results are under 5%. Note that the differences increase as the separation distance between windings increases; the largest difference occurs between winding 1 and 5. This is so because (3) is only applicable when the magnetic field is vertical and for large separations, the field curves a little. Therefore, it can be affirmed that not only can FEM be used to compute terminal leakage measurements, but that the obtained results are closer to reality than the formula.

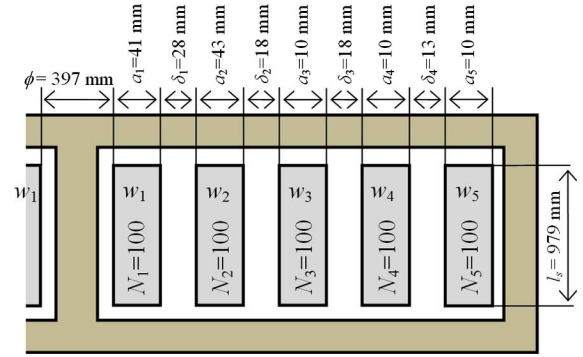


Fig. 2. Winding configuration of a five-layer transformer.

TABLE I
LEAKAGE INDUCTANCES FOR A FIVE-LAYER TRANSFORMER

Tests	Leakage Inductance [mH]		Difference [%]
	Formula (3)	FEM	
Test ₁₂	1.1019	1.0972	0.43
Test ₁₃	2.2161	2.2610	-2.03
Test ₁₄	2.8924	2.9908	-3.40
Test ₁₅	3.4713	3.6345	-4.70
Test ₂₃	0.8629	0.8655	-0.30
Test ₂₄	1.5910	1.6049	-0.87
Test ₂₅	2.2097	2.2534	-1.98
Test ₃₄	0.6785	0.6722	0.93
Test ₃₅	1.3317	1.3304	0.10
Test ₄₅	0.5823	0.5770	0.91

TABLE II
COMPUTED CURRENT FOR A FIVE-LAYER TRANSFORMER

Test	FEM (Fig. 2) Current [A]	Terminal Model (Fig. 3) Current [A]	Duality Model (Fig. 4) Current [A]	TDM (Fig. 12) Current [A]
Test ₁₂	2.9012	2.9010 (0.01%)	2.9010 (0.01%)	2.9010 (0.01%)
Test ₁₃	1.4078	1.4077 (0.01%)	1.6217 (-15.19%)	1.4077 (0.01%)
Test ₁₄	1.0643	1.0642 (0.01%)	1.2080 (-13.50%)	1.0642 (0.01%)
Test ₁₅	0.8758	0.8757 (0.01%)	0.9910 (-13.15%)	0.8757 (0.01%)
Test ₂₃	3.6776	3.6773 (0.01%)	3.6773 (0.01%)	3.6773 (0.01%)
Test ₂₄	1.9834	1.9832 (0.01%)	2.0699 (-4.36%)	1.9832 (0.01%)
Test ₂₅	1.4126	1.4125 (0.01%)	1.5051 (-6.55%)	1.4125 (0.01%)
Test ₃₄	4.7356	4.7352 (0.01%)	4.7352 (0.01%)	4.7352 (0.01%)
Test ₃₅	2.3925	2.3923 (0.01%)	2.5479 (-6.50%)	2.3923 (0.01%)
Test ₄₅	5.5163	5.5158 (0.01%)	5.5158 (0.01%)	5.5158 (0.01%)

III. TERMINAL AND DUALITY CIRCUITS

To compare the terminal and duality circuits, both models will be applied to the five-layer transformer shown in Fig. 2.

A. Existing Terminal Circuits

The first terminal equivalent circuits for multiwinding transformers are those proposed by Starr [28] and Boyajian [29], [30]. These models regularly contain negative inductances (see

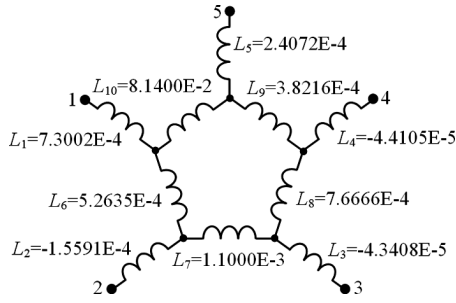


Fig. 3. Terminal model for the five-winding transformer (Fig. 2).

Fig. 3); therefore, precluding any physical identification of the circuit elements. There have been no problems reported using terminal models (with negative inductances) for steady-state calculations, but when used for transient simulations, these terminal models may produce numerical oscillations [31].

Fig. 3 shows the terminal equivalent circuit of the transformer in Fig. 2 (following [30]). The third column in Table II collects the currents calculated for the leakage inductance tests with the terminal model of Fig. 3. Differences between currents calculated with the terminal model and those computed with FEM are collected in parentheses in the third column of Table II. One can notice that the differences are very small (less than 0.6%). Therefore, it is possible to conclude that the model of Fig. 3 properly represents the terminal behavior of the multiwinding transformer of Fig. 2.

For the study of the electromagnetic transients, the most commonly used multiwinding (or multisection) transformer model is perhaps BCTRAN, which is included in the EMTP; see [32] and [33].

The BCTRAN model is based on the computation of the inverse leakage inductance matrix directly from standard tests at the transformer terminals. Therefore, the inversion of an ill-conditioned matrix is avoided. It is well known that the model is numerically stable for multiwinding transformers.

The main disadvantage of the BCTRAN transformer model, shared by all terminal models, is that the core geometry cannot be taken into account accurately. In fact, there are no internal nodes to connect the magnetizing branches. Therefore, the magnetizing phenomena are not considered properly. Magnetizing branches (including losses) are simply added across the winding closest to the core [33]. A detailed description of the BCTRAN model is out of the scope of this paper. Note, however, that the terminal behavior of the leakage inductance is stable and correct.

B. Existing Duality Derived Circuits

There are several variations of models obtained from the application of the principle of duality; see, for example, [1], [34], and [35]. An inductor (transversal to the flux) is used to represent each flux path, but the terminal behavior, in most cases, is not considered. Flux paths and, therefore, model topology are selected according to the phenomena that are to be studied.

Fig. 4 shows the duality model for the multilayer transformer of Fig. 2. The Table I column “Formula” shows the values of the leakage inductances ($LS_{i,j}$) of the duality model. The fourth

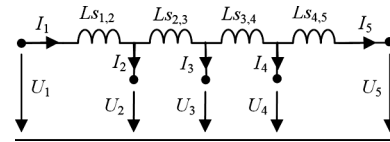


Fig. 4. Duality model for the five-winding transformer (Fig. 2).

column in Table II collects the currents calculated with the duality model of Fig. 4. Differences between currents calculated with the duality model and those computed with FEM are collected in parentheses in the fourth column of Table II. As can be seen from the results, this model does not properly reproduce the terminal response of the transformer even when the circuit elements (inductors) physically represent a leakage path in the window. Some of the errors are close to 15%.

IV. NEW TERMINAL-DUALITY CIRCUIT

In this section, a new circuit to model transformers with windings in any topology is proposed. The new circuit is derived from the application of the principle of duality between electric and magnetic equivalent circuits and simultaneously it is supported by both terminal-leakage measurements and short-circuit admittance measurements. Since the model unifies terminal models with models derived from duality, the new model is referred as the TDM. The TDM consists of a network of mutually coupled inductances that can be easily implemented into the environment of EMTP-type programs with readily available components.

The TDM model solves the most important limitations of existing models for multiwinding (or multisection) transformers. On one hand, the currently available duality models successfully establish a one-to-one relationship between the circuit elements and the building components of the transformer (core, windings, and insulation). However, duality models pay no attention to the terminal behavior and often there is a mismatch with terminal leakage measurements. On the other hand, terminal models accurately represent the behavior of the transformer leakage. However, the circuit elements cannot be related to the physical components of the transformer; therefore, they produce difficulties when trying to include the eddy current effects in the core and windings in the model and/or the nonlinear behavior of the core. The TDM can be retrofitted to include nonlinearities and eddy currents while preserving the physical meaning of all its components. This, however, is left for a sequel paper.

A. TDM for Layered Windings

To show the methodology used to create the TDM, the geometry of a transformer with n -concentric windings arranged in layers is chosen (see Fig. 5). A reluctance circuit has been drawn in Fig. 5. It represents the magnetizing flux path with n reluctances R_m and the leakage flux paths with $n-1$ reluctances R that are set in the transformer. Then, the principle of duality is applied, and the inductance circuit is obtained as shown in Fig. 6. To be in the position of fully and properly estimating the behavior of a transformer with n windings, the model must have at least $n \cdot (n-1)/2$ elements (or degrees of freedom) according to the Boyajian rule [29]. To complement the TDM

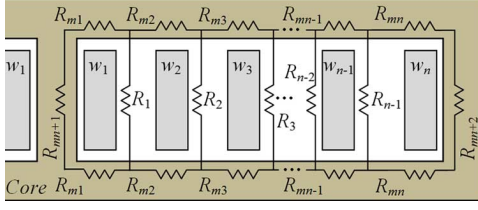


Fig. 5. Phase reluctance circuit for the multilayer transformer including core and air paths.

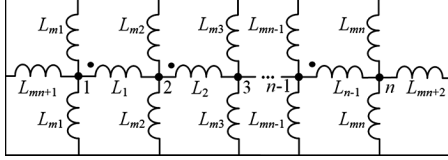


Fig. 6. Phase inductance circuit including the magnetizing (core) and leakage (air) elements.

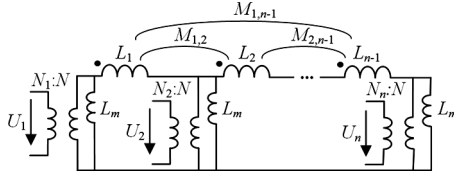


Fig. 7. Phase electrical circuit of the TDM for a multilayer or multidisk windings including magnetizing and leakage elements.

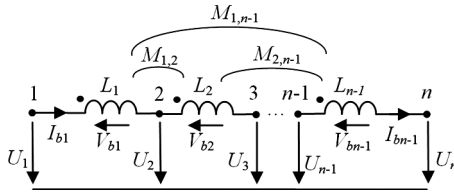


Fig. 8. Phase leakage electric circuit of the TDM for multilayer or multidisk windings.

model, one can take into account the mutual couplings between the inductors. It has been shown in [24] that the mutual couplings physically represent the thickness on the windings not energized during the short-circuit tests. The complete electrical circuit of TDM, including the magnetizing branches, is shown in Fig. 7, where N_1, N_2, \dots, N_n are the number of turns in each winding and N is the number of turns taken as reference.

In this paper, magnetizing branches are not considered except, as shown in Fig. 7, to mark the connection points between the two dual models (leakage and magnetizing).

The TDM for the transformer leakage is obtained from the duality model and adding the mutual couplings as shown in Fig. 8.

The remainder of this section is dedicated to compute the parameters of the circuit from terminal tests. The electric circuit of the TDM of Fig. 8 must satisfy Kirchoff's voltage law (KVL) expressed as follows:

$$V_{bk} = j\omega \sum_{p=1}^{n-1} M_{k,p} I_{bp}; \quad k = 1, \dots, n-1 \quad (4)$$

where V_{bk} is the voltage drop across branch k , I_{bp} is the current flowing through branch p , and M_{kp} is the mutual inductance between branches k and p .

Self-inductances L_k and mutual inductances $M_{k,p}$ of the TDM for a multilayer transformer are calculated from the leakage inductances obtained from the standard leakage impedance tests (1). Considering (4), the voltage of node i to ground (U_i) is calculated as

$$U_i = \sum_{k=i}^{j-1} V_{bk} = j\omega \sum_{k=i}^{j-1} \sum_{p=1}^{n-1} M_{k,p} I_{bp}. \quad (5)$$

Looking at the circuit of Fig. 8, one can realize that during a short-circuit test between two windings (nodes in the dual circuit), only the inductors contained within the testing points carry current. For example, when testing between points 1 and 2, only L_1 carries current. When testing between points 1 and 3, L_1 and L_2 carry current, but no current circulates in the other inductors. This fact can be generalized as follows:

$$I_i = I_j = I_m; I_q = 0 \\ i < m < j; q < i, q > j; i, j, m, q = 1, \dots, n-1. \quad (6)$$

Substituting (6) into (5), we obtain

$$U_i = j\omega \left(\sum_{k=i}^{j-1} \sum_{p=i}^{j-1} M_{k,p} \right) I_i \quad (7)$$

and the expression of the leakage inductance $L_{s_{i,j}}$ as a function of the inductances of TDM becomes

$$L_{s_{i,j}} = \frac{U_i}{j\omega I_i} = \sum_{k=i}^{j-1} L_k + 2 \left(\sum_{k=i}^{j-2} \sum_{p=k+1}^{j-1} M_{k,p} \right) \\ i < j; i, j = 1, \dots, n-1. \quad (8)$$

Substituting $j = i + 1$ in (8), the self-inductances L_i in the TDM are

$$L_i = L_{s_{i,i+1}}; \quad i = 1, \dots, n-1. \quad (9)$$

From (9), one can see that the self-inductances of the TDM are computed directly from the leakage inductance tests between two consecutive windings. This is in full agreement with the principle of duality since these inductances represent the paths of leakage flux between the two windings.

Substituting $j = i + 2$ in (8), we obtain

$$L_{s_{i,i+2}} = L_i + L_{i+1} + 2M_{i,i+1}. \quad (10)$$

Substituting L_i and L_{i+1} in (10) by $L_{s_{i,i+1}}$ and $L_{s_{i+1,i+2}}$ using (9), and adding an auxiliary zero term $L_{s_{i+1,i+1}} = 0$ to (10), we obtain the following expression to compute $M_{i,i+1}$:

$$M_{i,i+1} = \frac{1}{2} (L_{s_{i,i+2}} + L_{s_{i+1,i+1}} - L_{s_{i,i+1}} - L_{s_{i+1,i+2}}). \quad (11)$$

Substituting $j = i + 3$ in (8) yields

$$L_{s_{i,i+3}} = L_i + L_{i+1} + L_{i+2} + 2(M_{i,i+1} + M_{i+1,i+2} + M_{i,i+2}). \quad (12)$$

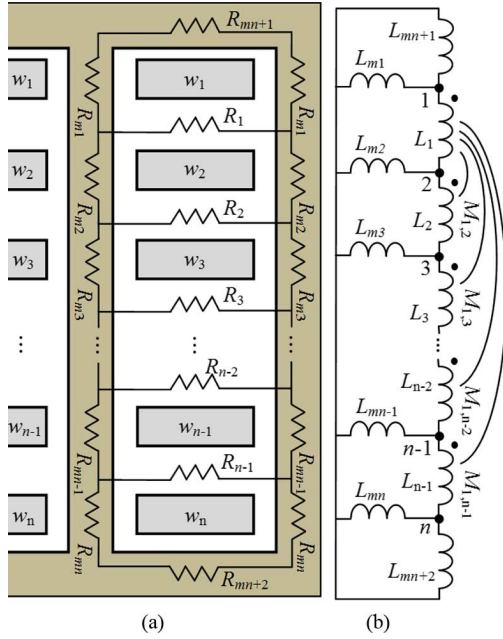


Fig. 9. (a) Phase reluctance circuit (including core and air paths). (b) Phase inductance circuit for the multidisk transformer (including leakage and magnetization).

Substituting L_i , L_{i+1} , and L_{i+2} in (12) by (9) and replacing $M_{i,i+1}$ and $M_{i+1,i+2}$ in (12) by (11), $M_{i,i+2}$ can be calculated as

$$M_{i,i+2} = \frac{1}{2} (Ls_{i,i+3} - Ls_{i,i+1} - Ls_{i+1,i+2} - Ls_{i+2,i+3} - Ls_{i,i+2} + Ls_{i,i+1} + Ls_{i+1,i+2} - Ls_{i+1,i+3} + Ls_{i+1,i+2} + Ls_{i+2,i+3}). \quad (13)$$

Simplifying terms in (13), one gets

$$M_{i,i+2} = \frac{1}{2} (Ls_{i,i+3} + Ls_{i+1,i+2} - Ls_{i,i+2} - Ls_{i+1,i+3}). \quad (14)$$

Comparing (11) and (14), the calculation of the mutual inductances $M_{i,j}$ in the TDM can be generalized as follows:

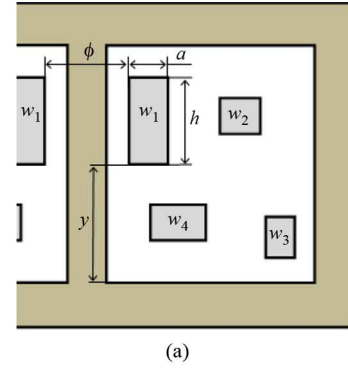
$$M_{i,j} = \frac{1}{2} (Ls_{i,j+1} + Ls_{i+1,j} - Ls_{i,j} - Ls_{i+1,j+1}). \quad (15)$$

Equation (15) is consistent with the expressions found in [24] and [29] to compute the mutual couplings and negative inductances, respectively, for three-winding transformers.

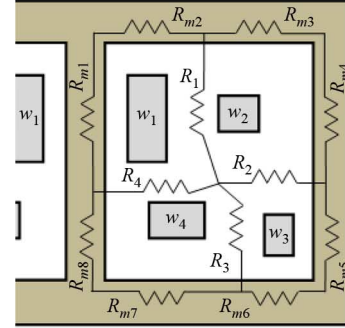
The TDM model is now complete and all of its elements can be computed from leakage tests and using (9) and (15).

B. TDM for Disk Windings

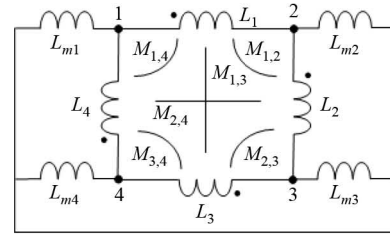
The same methodology described before for layer-type windings can be applied directly to implement the TDM in transformers with disk-type windings. According to Fig. 9(a), the $n - 1$ leakage magnetic flux paths between discs is set within the transformer window. Consequently, the inductance circuit of Fig. 9(b) is obtained. The topology of the leakage inductance circuit is the same as the circuit of Fig. 6. Therefore, the electric circuit of the TDM for the multidisk transformer is shown in Fig. 8.



(a)



(b)



(c)

Fig. 10. (a) Window geometry. (b) Phase reluctance circuit of a four non-concentric winding transformer per phase (including core and air elements). (c) Phase electric circuit of the TDM for a four nonconcentric winding transformer (including magnetizing and leakage elements).

C. TDM for Windings With General Topology

The TDM can be applied to arbitrary winding topologies. Take, for example, the nonconcentric four-winding transformer shown in Fig. 10(a). It can be seen that there is no symmetry, and the windings (or sections) do not have uniform dimensions or spacing. Here, four leakage flux paths can be distinguished, resulting in the duality part of the model as shown in Fig. 10(b). Thus, four mutually coupled inductances form the electric circuit of the TDM as illustrated in Fig. 10(c).

The self-inductances of the model are calculated from the standard leakage inductance tests (experimentally measured or numerically computed by FEM simulations). In order to be in full agreement with the principle of duality, each pair of consecutive windings must fulfill the following expression:

$$L_1 = Ls_{1,2}; L_2 = Ls_{2,3}; L_3 = Ls_{3,4}; L_4 = Ls_{1,4} \quad (16)$$

where L_i is the self inductance of the inductor i in the TDM circuit, and $Ls_{i,j}$ is obtained from the leakage inductance test between the windings i and j . Note that it is also possible to

obtain the leakage inductances from the geometrical dimensions of the windings and spacing.

In this irregular case, the calculation of mutual inductances does not have an analytical expression because the equations system, which is obtained by applying the standard leakage impedance tests (1) to the TDM, is indeterminate. However, the mutual inductances can be conveniently obtained from short-circuit admittance tests so that the model accurately reproduces the terminal behavior of the transformer. The short-circuit admittance tests satisfy the following expression:

$$\mathbf{Y}_n \mathbf{V}_n = \mathbf{I}_n \quad (17)$$

where \mathbf{V}_n is the nodal vector of terminal voltages (with respect to reference) and \mathbf{I}_n is the nodal vector of currents flowing through the windings. The elements of the nodal admittance matrix \mathbf{Y}_n are the admittances computed (or measured) using (2) from short-circuit tests.

In addition, the TDM satisfies the following branch-node transformation (matrix) equations:

$$\mathbf{V}_b = \mathbf{Z}_b \mathbf{I}_b \quad (18)$$

$$\mathbf{I}_b = \mathbf{Z}_b^{-1} \mathbf{V}_b \quad (19)$$

$$\mathbf{A}^T \mathbf{I}_b = \mathbf{I}_n, \quad \mathbf{V}_b = \mathbf{A} \mathbf{V}_n \quad (20)$$

$$\mathbf{I}_n = \mathbf{A}^T \mathbf{Z}_b^{-1} \mathbf{A} \mathbf{V}_n \quad (21)$$

where \mathbf{Z}_b is the branch impedance matrix of the TDM, \mathbf{V}_b and \mathbf{I}_b are the branch vector of the voltages and currents, and \mathbf{A} is the incidence matrix (node element). Combining (17) and (21), the relationship between \mathbf{Z}_b (the branch impedance matrix) of the TDM and the short-circuit admittance matrix is given by

$$\mathbf{Y}_n = \mathbf{A}^T \mathbf{Z}_b^{-1} \mathbf{A}. \quad (22)$$

Neglecting the resistive part of the branch impedance, the following expression is obtained:

$$\mathbf{Y}_n = \mathbf{A}^T (j\omega \mathbf{L})^{-1} \mathbf{A} \quad (23)$$

where \mathbf{L} is the branch (leakage) inductance matrix of the TDM. The mutual inductances of \mathbf{L} ($M_{i,j}$) are obtained numerically from (23). For this, an error function \mathbf{F} is defined to search for the minimum error in the solution of (23) as

$$\mathbf{F} = \mathbf{A}^T (j\omega \mathbf{L})^{-1} \mathbf{A} - \mathbf{Y}_n \quad (24)$$

The nonlinear system of (24) is solved iteratively, using, for instance, the least squares routine in Matlab. The solution process starts from an initial matrix \mathbf{L}_0 defined as follows:

$$\mathbf{L}_0 = \begin{pmatrix} L_{s12} & 0 & 0 & 0 \\ 0 & L_{s23} & 0 & 0 \\ 0 & 0 & L_{s34} & 0 \\ 0 & 0 & 0 & L_{s14} \end{pmatrix}. \quad (25)$$

Thus, the solution to \mathbf{L} in (23) is reached when the value of the error function \mathbf{F} is less than a small tolerance chosen by the user. For example, in the general case studied in Section V-C, the experience of the authors is that when fixing a relative error smaller than 10^{-12} , the solution converges within 20 iterations successfully.

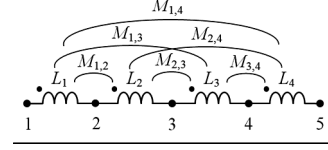


Fig. 11. Leakage electric circuit of the TDM for five concentric windings.

V. ILLUSTRATION EXAMPLES

A. Layer Winding

In this section, the leakage inductance matrix of the TDM is calculated for the transformer of Fig. 2. The equivalent electric circuit of the TDM is shown in Fig. 11. Table I (second column) shows the leakage obtained by 2-D-FEM simulations. After applying (9) for the self-elements and (15) for the mutual elements, the inductance matrix becomes

$$\mathbf{L} = \begin{pmatrix} 1.0972 & 0.1492 & -0.0048 & -0.0024 \\ 0.1492 & 0.8655 & 0.0336 & -0.0049 \\ -0.0048 & 0.0336 & 0.6722 & 0.0406 \\ -0.0024 & -0.0049 & 0.0406 & 0.5770 \end{pmatrix} \times 10^{-3}. \quad (26)$$

The standard leakage inductance test of Fig. 1(a) was implemented to the circuit of Fig. 11 in Simulink. Tests conditions(1) are imposed to the circuit to calculate the currents. Then, the accuracy of the TDM is compared with the currents computed with 2-D-FEM. The fifth column of Table II collects the currents calculated by TDM of Fig. 11. The differences between the currents are in parentheses. One can see an almost perfect match (maximum difference under 0.01%).

One can use the leakage inductance matrix (26) to compute the induced voltage in the windings. For example, if winding 2 is energized and there is a load connected to winding 1 (with all other windings in open circuit), the voltage induced in windings 3, 4, and 5 is larger than the voltage applied to winding 2 (in per unit). This occurs because the induced voltage is proportional to the flux that a winding links and the leakage flux is in the same direction as the main (magnetizing) flux in the core. In the Appendix, we show that under the aforementioned test, all external windings link more flux lines than the internal winding 2 by a factor of (a_2 is the thickness of winding 2)

$$\frac{\mu_0 N^2 I}{l_s} \left(\frac{a_2}{6} \right). \quad (27)$$

B. Disk Winding

The geometric dimensions of a disk winding are shown in Fig. 12. The electric equivalent circuit for the leakage inductance of the TDM is shown in Fig. 11. Table III shows the inductances obtained from the leakage tests from 2-D-FEM simulations. The leakage inductance matrix is obtained from (9) and (15) as in the previous case, yielding

$$\mathbf{L} = \begin{pmatrix} 3.1302 & 0.3179 & -0.0395 & -0.0205 \\ 0.3179 & 3.1118 & 0.3095 & -0.0413 \\ -0.0395 & 0.3095 & 3.1115 & 0.3182 \\ -0.0205 & -0.0413 & 0.3182 & 3.1299 \end{pmatrix} \times 10^{-3}. \quad (28)$$

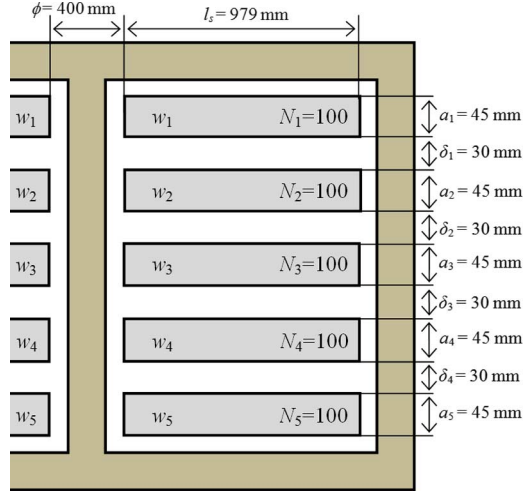


Fig. 12. Geometry of a five-disks transformer.

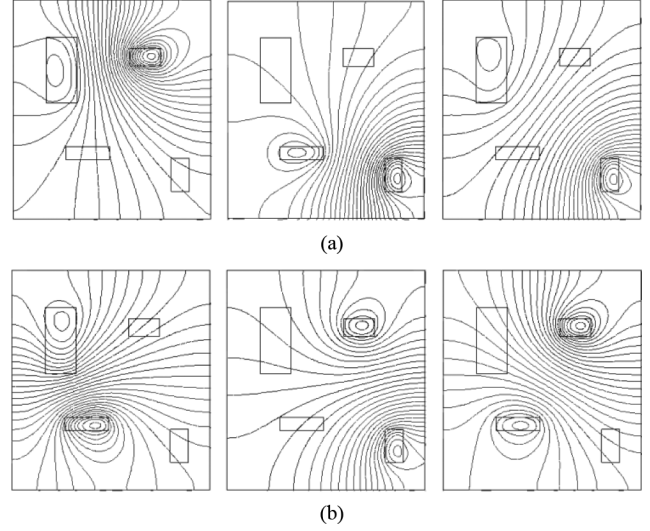

 Fig. 13. 2-D-FEM magnetic flux distribution during leakage tests. (a) Test to determine L_{s12} , L_{s34} , and L_{s13} . (b) Test to determine L_{s14} , L_{s23} , and L_{s24} .

 TABLE III
CURRENT AND LEAKAGE INDUCTANCE OF THE FIVE-DISK TRANSFORMER

Tests	Leakage Inductance [mH]	FEM Current [A]	TDM Current [A]	Difference [%]
Test ₁₂	3.1302	1.0169	1.0168	0.01
Test ₁₃	6.8779	0.4628	0.4628	0.00
Test ₁₄	10.5296	0.3023	0.3023	0.00
Test ₁₅	14.1723	0.2246	0.2246	0.00
Test ₂₃	3.1118	1.0229	1.0228	0.01
Test ₂₄	6.8424	0.4652	0.4652	0.00
Test ₂₅	10.5261	0.3024	0.3024	0.00
Test ₃₄	3.1115	1.0230	1.0229	0.01
Test ₃₅	6.8779	0.4628	0.4628	0.00
Test ₄₅	3.1299	1.0170	1.0169	0.01

To check the accuracy of the obtained TDM for the transformer of Fig. 12, the TDM is implemented in Simulink, and the tests of Fig. 1(a) corresponding to (1) are performed. Currents calculated by TDM and those computed by 2-D-FEM are compared in Table III. The differences are negligible.

C. General Winding

The TDM is obtained for the general topology transformer shown in Fig. 10(a). Table IV shows the geometric dimensions of the transformer. The magnetic flux distributions of the leakage tests between each pair of windings are plotted in Fig. 13. The leakage inductances obtained by the 2-D-FEM model are collected in the second column of Table V. The nodal admittance matrix obtained from the short-circuit tests obtained with 2-D-FEM are

$$Y_n = \begin{pmatrix} 46.3071 & -16.6820 & -1.6824 & -27.8898 \\ -16.6820 & 24.2791 & -3.8389 & -3.7565 \\ -1.6824 & -3.8389 & 15.3188 & -9.7950 \\ -27.8898 & -3.7565 & -9.7950 & 41.4652 \end{pmatrix}. \quad (29)$$

 TABLE IV
GEOMETRIC DIMENSIONS OF THE GENERAL WINDINGS TRANSFORMER

winding	h [mm]	a [mm]	ϕ [mm]	y [mm]	N
1	150	70	320	340	10
2	40	70	700	370	10
3	75	40	860	100	10
4	30	100	440	150	10

 TABLE V
CURRENT AND LEAKAGE INDUCTANCE OF THE GENERAL WINDINGS TRANSFORMER

Tests	Leakage Inductance [mH]	FEM Current [A]	TDM Current [A]	Difference [%]
Test ₁₂	0.1428	22.2889	22.2260	0.28
Test ₁₃	0.2623	12.1352	12.0726	0.51
Test ₁₄	0.0948	33.5765	33.5388	0.11
Test ₂₃	0.3019	10.5450	10.5097	0.33
Test ₂₄	0.1875	16.9745	16.9688	0.03
Test ₃₄	0.2245	14.1762	14.1750	0.01

The incidence matrix (30) is obtained by inspection of Fig. 10(c) as

$$A = \begin{pmatrix} 1 & -1 & 0 & 0 \\ 0 & 1 & -1 & 0 \\ 0 & 0 & 1 & -1 \\ -1 & 0 & 0 & 1 \end{pmatrix}. \quad (30)$$

Then, the self-inductances of the TDM for this transformer are calculated from (16), and the mutual inductances are computed from (24) using as initial conditions (25). The results of the minimization process are given by the following expression:

$$L = \begin{pmatrix} 0.1428 & -0.0918 & -0.0267 & -0.0255 \\ -0.0918 & 0.3019 & -0.1699 & -0.0420 \\ -0.0267 & -0.1699 & 0.2245 & -0.0279 \\ -0.0255 & -0.0420 & -0.0279 & 0.0948 \end{pmatrix} \times 10^{-3}. \quad (31)$$

The electric circuit of the TDM was implemented in Simulink to compute the current of the standard leakage tests (1). The

TABLE VI
RESULTS OF THE INDUCED VOLTAGE TEST

	Winding				
	1	2	3	4	5
Voltage [V]	945.3	1000	1015.3	1014.8	1014.5
Current [A]	945.3	945.3	0	0	0

accuracy of the TDM is examined by comparing the current obtained with 2-D-FEM as shown in Table V. The differences are less than 0.5%.

VI. CONCLUSION

This paper has presented a new equivalent circuit for the representation of the leakage inductance of multiwinding (applicable to multisection) transformers. Its most important feature is that terminal and duality derived models are now unified and all circuit elements have a clear physical meaning as flux paths in the transformer window and simultaneously the terminal behavior is properly represented.

The circuit consists of a set of mutually coupled inductors. In contrast with other methods, the elements of our model are available in any circuit simulation program. This is of particular significance for transient studies since mutually coupled inductors are readily available in all EMTP-type simulation programs.

The circuit elements can be computed in three ways yielding identical results: from design formulas, finite-element simulations, or terminal short-circuit measurements.

A number of examples, ranging from layer, disk, and arbitrary winding designs have been presented for illustration of the model. The validation of the model has been carried out by comparing the currents computed with the obtained circuit by simulating the standard tests against 2-D-FEM simulations.

It is believed that the physical meaning of the self-inductors would enable proper modeling of eddy current effects directly in the circuit. We intend to continue our research in that path and present the results in a sequel paper.

APPENDIX STUDY OF THE INDUCED VOLTAGE

In this section, we analyze the induced voltage of the five-winding (layer-type) transformer using the leakage inductance matrix (26). The test consists in energizing winding 2, connecting a load to winding 1, and leaving all other windings (3–5) in open circuit. Figs. 7 and 8 help us visualize the circuit and testing conditions.

We apply a voltage source $U_2 = 1.0$ kV to winding 2, connect a load of $R = 1 \Omega$ to winding 1, and compute the voltage and current at the terminals of all windings. Table VI shows the results of the load test. One can detect that the voltage of windings 3–5 is higher than the voltage of the excited winding 2. For corroboration, finite-element simulations were performed yielding identical results.

To explain these results, we rely on Fig. 14 which shows the idealized distribution of the magnetic flux during this test. We note that because the energized winding is number 2, all of the flux (magnetizing and leakage) is upwards. In the figure, we also include the trapezoidal distribution of the leakage flux as reference.

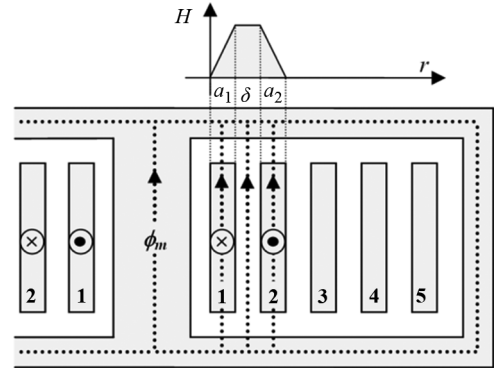


Fig. 14. Idealized magnetic flux distribution during load tests.

Using (3) and Fig. 14, we can obtain expressions for the linked flux for each winding. Winding 1 links the magnetizing flux and partially the leakage flux over winding 1, yielding

$$\phi_1 = \phi_m + \frac{\mu_0 N^2 I}{l_s} \left(\frac{a_1}{3} \right). \quad (32)$$

Winding 2 links all of the internal flux (magnetizing, leakage over winding 1, and the flux in-between the windings) plus a part of the leakage flux over winding 2, giving

$$\phi_2 = \phi_m + \frac{\mu_0 N^2 I}{l_s} \left(\frac{a_1}{2} + \delta + \frac{a_2}{3} \right). \quad (33)$$

Note that the denominator of a_1 in (33) is 2 while in (32), it is 3. This is because winding 2 links the flux over winding 2 fully, while winding 1 links only this flux partially. Similarly, all external windings (3–5) link the following flux:

$$\phi_3 = \phi_4 = \phi_5 = \phi_m + \frac{\mu_0 N^2 I}{l_s} \left(\frac{a_1}{2} + \delta + \frac{a_2}{2} \right). \quad (34)$$

Subtracting (33) from (34), we obtain

$$\phi_3 - \phi_2 = \frac{\mu_0 N^2 I}{l_s} \left(\frac{a_2}{2} - \frac{a_2}{3} \right) = \frac{\mu_0 N^2 I}{l_s} \left(\frac{a_2}{6} \right). \quad (35)$$

We note that all of the external windings link more flux than the energized winding 2. Therefore, the induced voltage in windings 3–5 is higher than the voltage of winding 2. The small differences between the voltages of windings 3–5 are caused by the fact that the actual distribution of the leakage flux is not exactly as shown in Fig. 14, but reasonably close.

REFERENCES

- [1] F. de León, P. Gómez, J. A. Martínez-Velasco, and M. Rioual, "Chapter 4, Transformers," in *Power System Transients: Parameter Determination*, J. A. Martínez-Velasco, Ed. Boca Raton, FL: CRC, 2009, pp. 177–250.
- [2] J. A. Martínez and B. Mork, "Transformer modeling for low-and mid-frequency transients—a review," *IEEE Trans. Power Del.*, vol. 20, no. 2, pt. 2, pp. 1525–1632, Apr. 2005.
- [3] J. A. Martínez, R. Walling, B. A. Mork, J. Martín-Arnedo, and D. Durbak, "Parameter determination for modeling system transients-part III: Transformers," *IEEE Trans. Power Del.*, vol. 20, no. 3, pp. 2051–2062, Jul. 2005.
- [4] X. M. Lopez-Fernandez and C. Álvarez-Mariño, "Computation method for transients in power transformers with lossy windings," *IEEE Trans. Magn.*, vol. 45, no. 3, pp. 1863–1866, Mar. 2009.

- [5] W. J. Mc Nutt, T. J. Blalock, and R. A. Hinton, "Response of transformer windings to system transient voltages," *IEEE Trans. Power App. Syst.*, vol. PAS-93, no. 2, pp. 457–466, Mar./Apr. 1974.
- [6] A. S. Al-Fuhaid, "Frequency characteristics of single phase two winding transformer using distributed parameter modeling," *IEEE Trans. Power Del.*, vol. 16, no. 4, pp. 637–642, Oct. 2001.
- [7] L. Rabins, "A new approach to the analysis of impulse voltages and gradients in transformer windings," *AIEE Trans.*, vol. 79, no. 4, pp. 1784–1791, Feb. 1960.
- [8] Y. Shibuya, S. Fujita, and N. Hosokawa, "Analysis of very fast transient overvoltage in transformer winding," *Proc. Inst. Elect. Eng., Gen. Transm. Distrib.*, vol. 144, no. 5, pp. 461–468, Sep. 1997.
- [9] Y. Shibuya, S. Fujita, and E. Tamaki, "Analysis of very fast transients in transformer," *Proc. Inst. Elect. Eng., Gen. Transm. Distrib.*, vol. 148, no. 5, pp. 377–383, Sep. 2001.
- [10] M. Popov, L. van der Sluis, and G. C. Paap, "Computation of very fast transient overvoltages in transformer windings," *IEEE Trans. Power Del.*, vol. 18, no. 4, pp. 1268–1274, Oct. 2003.
- [11] G. Liang, H. Sun, X. Zhang, and X. Cui, "Modeling of transformer windings under very fast transient overvoltages," *IEEE Trans. Electromagn. Compat.*, vol. 48, no. 4, pp. 621–627, Nov. 2006.
- [12] M. Popov, L. van der Sluis, R. P. P. Smeets, and J. L. Roldan, "Analysis of very fast transients in layer-type transformer windings," *IEEE Trans. Power Del.*, vol. 22, no. 1, pp. 238–247, Jan. 2007.
- [13] S. M. H. Hosseini, M. Vakilian, and G. B. Gharehpetian, "Comparison of transformer detailed models for fast and very fast transient studies," *IEEE Trans. Power Del.*, vol. 23, no. 2, pp. 733–741, Apr. 2008.
- [14] A. Miki, T. Hosoya, and K. Okuyama, "A calculation method for impulse voltage distribution and transferred voltage in transformer windings," *IEEE Trans. Power App. Syst.*, vol. PAS-97, no. 3, pp. 930–939, May/June. 1978.
- [15] D. J. Wilcox and T. P. McHale, "Modified theory of modal analysis for the modeling of multiwinding transformers," *Proc. Inst. Elect. Eng., Gen. Transm. Distrib.*, vol. 139, no. 6, pp. 505–512, Nov. 1992.
- [16] K. Ragavan and L. Satish, "An efficient method to compute transfer function of a transformer from its equivalent circuit," *IEEE Trans. Power Del.*, vol. 20, no. 2, pt. 1, pp. 780–788, Apr. 2005.
- [17] B. Gustavsen, "Wide band modeling of power transformers," *IEEE Trans. Power Del.*, vol. 19, no. 1, pp. 414–422, Jan. 2004.
- [18] P. I. Fergestad and T. Henriksen, "Transient oscillations in multiwinding transformers," *IEEE Trans. Power App. Syst.*, vol. PAS-93, no. 2, pp. 500–509, Mar./Apr. 1974.
- [19] F. de León and A. Semlyen, "Complete transformer model for electromagnetic transients," *IEEE Trans. Power Del.*, vol. 9, no. 1, pp. 231–239, Jan. 1994.
- [20] F. de León and A. Semlyen, "Reduced order model for transformer transients," *IEEE Trans. Power Del.*, vol. 7, no. 1, pp. 361–369, Jan. 1992.
- [21] F. de León and A. Semlyen, "Detailed modeling of eddy current effects for transformer transients," *IEEE Trans. Power Del.*, vol. 9, no. 2, pp. 1143–1150, Apr. 1994.
- [22] R. M. Del Vecchio, "Applications of a multiterminal transformer model using two winding leakage inductances," *IEEE Trans. Power Del.*, vol. 21, no. 3, pp. 1300–1308, Jul. 2006.
- [23] R. M. Del Vecchio, "Multiterminal three phase transformer model with balanced or unbalanced loading," *IEEE Trans. Power Del.*, vol. 23, no. 3, pp. 1439–1447, Jul. 2008.
- [24] F. de León and J. A. Martínez, "Dual three-winding transformer equivalent circuit matching leakage measurements," *IEEE Trans. Power Del.*, vol. 24, no. 1, pp. 160–168, Jan. 2009.
- [25] *IEEE Standard Test Code for Liquid-Immersed Distribution, Power, and Regulating Transformers*, IEEE Standard C57.12.90-2006, 2006.
- [26] Flux 2D (Version 10.4). 2011. [Online]. Available: <http://www.cedrat.com/en/software-solutions/flux.html>
- [27] K. Karsai, D. Kerényi, and L. Kiss, *Large Power Transformers*. New York: Elsevier, 1987.
- [28] F. Starr, "Equivalent circuits—I," *AIEE Trans.*, vol. 57, pp. 287–298, Jun. 1932.
- [29] A. Boyajian, "Theory of three-circuit transformers," *AIEE Trans.*, pp. 208–528, Feb. 1924.
- [30] L. F. Blume, A. Boyajian, G. Camilli, T. C. Lennox, S. Minneci, and V. M. Montsinger, *Transformer Engineering*, A. Boyajian, Ed. New York: Wiley, 1951, ch. V.
- [31] X. Chen, "Negative inductance and numerical instability of the saturable transformer component in EMTP," *IEEE Trans. Power Del.*, vol. 15, no. 4, pp. 1199–1204, Oct. 2000.
- [32] V. Brandwajn, H. W. Dommel, and I. I. Dommel, "Matrix representation of three-phase n-winding transformers for steady-state and transient studies," *IEEE Trans. Power App. Syst.*, vol. PAS-101, no. 6, pp. 1369–1378, Jun. 1982.
- [33] H. W. Dommel, *EMTP Theory Book*. Portland, OR: Bonneville Power Administration, 1986.
- [34] G. Slemmon, *Electric Machines and Drives*. Reading, MA: Addison-Wesley, 1992.
- [35] N. Chiesa, B. A. Mork, and H. K. Høidalen, "Transformer model for inrush current calculations: Simulations, measurements and sensitivity analysis," *IEEE Trans. Power Del.*, vol. 25, no. 4, pp. 2599–2608, Oct. 2010.



Casimiro Álvarez-Mariño received the M.Sc. (Hons.) degree in electrical engineering from Vigo University, Vigo, Spain, in 2006, where he is currently pursuing the Ph.D. degree in electrical engineering, developing research on very fast transient overvoltages in transformers.

He was on a study leave at the Polytechnic Institute of New York University in 2010. He is collaborating in research projects for Spanish and Portuguese utilities and power transformer manufacturers. His research interests are in the modeling and simulation of electromagnetic transient and steady-state analysis applied to the design of electrical devices.



Francisco de León (SM'02) received the B.Sc. and M.Sc. (Hons.) degrees in electrical engineering from the National Polytechnic Institute (Mexico), in 1983 and 1986 respectively, and the Ph.D. degree from the University of Toronto, Toronto, ON, Canada, in 1992.

Currently, he is an Associate Professor at Polytechnic Institute of NYU, Brooklyn, NY. He has held several academic positions in Mexico and has worked for the Canadian electric industry. His research interests include the definition of powers under nonsinusoidal conditions, the transient and steady-state analyses of power systems, the thermal rating of cables and transformers, and the calculation of the electromagnetic field applied to machine design and modeling.



Xose M. López-Fernández (M'96) received the M.Sc. degree in electrical engineering and the Ph.D. degree in electrical engineering (Hons.) from Vigo University, Vigo, Spain, in 1992 and 1997, respectively.

Currently, he is a Professor in the Department of Electrical Engineering, University of Vigo, and was a Visiting Professor at the University of Artois, Béthune, France. He is the Publisher and Co-Editor of the e-monograph *Transformers in Practice*. His research interests are on design aspects of electrical machines.

Prof. Lopez-Fernandez is the General Chairman of The International Advanced Research Workshop on Transformers. He is leading research projects for the Spanish and Portuguese utilities and power transformer manufacturers. He received the Alfons Hoffmann's Medal from the Polish Power Engineering Society in 2004. He is a member of the IEEE–Power and Energy Society Transformers Committee.